SPECTRAL SIMULATION ON REMOTE SENSING REFLECTANCE OF PETROLEUM-CONTAMINATED WATER BODY USING HYDROLIGHT

Junjie Yang (1), Miaofen Huang (1, *), Weijian Luo (1), Yang Zhuang (1), Bingcai Chen (1), Zhonglin Wang (1)

[1] Guangdong Ocean University, No. 1 Haida Road, Mazhang District, Zhanjiang, 524088, China
Email: junjie_y@foxmail.com; hmf808@163.com; lwjluo@sina.com; zhuangyang826@foxmail.com;
bingcai.chen.0548@gmail.com; wzllin@126.com
*Corresponding author：hmf808@163.com

KEY WORDS: Hydrolight, normalized remote sensing reflectance, petroleum-contaminated water body, spectral simulation

ABSTRACT: A survey was conducted to collect data at Dalian Port which is located in the south of Liaoning province, China and its adjacent sea area from August 25th to 27th, 2018, in order to describe the relations between remote sensing reflectance (R_{rs}) and petroleum concentration, specific absorption coefficient and specific backscattering coefficient in petroleum-contaminated water body. Three simulation tests were designed to help Hydrolight simulate R_{rs} of petroleum-contaminated water or pure water in specified physical environments. They are denoted as TEST I, TEST II and TEST III respectively. From the simulation tests, three conclusions are drawn here. 1) In TEST I, by fixing specific absorption coefficient and specific backscattering coefficient, and changing the petroleum concentration, R_{rs} decreases with the increase of petroleum concentration between 420 to 476 nm, but increases with the increase of petroleum concentration in the wavelength range of 476 to 600 nm; by fixing the petroleum concentration and specific backscattering coefficient, and changing specific absorption coefficient , R_{rs} decreases with the increase of the specific absorption coefficient in the whole study wavelength range (420~600 nm); however R_{rs} increases with the increase of the specific backscattering coefficient when fixing the petroleum concentration and specific absorption coefficient, and changing specific backscattering coefficient. 2) Following TEST I, the method used in TEST II by fixing two parameters and randomly choosing a group of *in-situ* data that vary with station and depth (or wavelength) as the last parameter's data proves the conclusions made by 1) again, and makes further efforts to reveal that the specific absorption coefficient contributes more to R_{rs} than petroleum concentration and specific backscattering coefficient. 3) TEST III takes the method in TEST I again to fix the specific absorption coefficient and the specific backscattering coefficient. In this case, the petroleum concentration can come down to zero compared with the method in TEST I. Results of this case shows that R_{rs} of petroleum-contaminated water body and pure water body can be clearly distinguished in the blue-green bands (430-560 nm), and normalized R_{rs} has better performance to identify the petroleum-contaminated water from pure water, especially in the green band (500-560 nm).

1. INTRODUCTION

Petroleum-pollutants can be considered as one form of organic pollutants in water body (Huang et al., 2012). And petroleum-pollutants turn up in various forms in the marine environment: as aerosols and free molecules in the atmosphere, as oil layers and emulsions on the water surface, as emulsions, suspensions and dissolved phases in the water column and on the bottom sediments (Król et al, 2006). In recent years, petroleum-pollution became serious day by day. While conventional marine observation techniques cannot match environmental processes in the upper ocean over extended spatial and temporal scales (Novo et al., 1991; Huang et al., 2009, 2012). Satellite remote sensing of ocean reflectance is a unique tool for studying environmental processes in the upper ocean since the technology possesses the advantages of low-cost, regional and global, long-term monitoring, and of real-time or timely observation (Tan and Shao, 2000; Wozniak and Stramski, 2004), and also can be used for continual monitoring of marine organic pollutants over large spatial and temporal scales. Previous studies have shown that the monitoring of oil layers by remote sensing on the petroleum-contaminated seawater surface has been paid close attention for many years, whereas petroleum pollution that oil layer has not developed seldom be considered at present (Huang et al, 2015). Huang, et al. (2016) still suggested that petroleum-pollutants in the water column can be considered as a water constituent, then ocean color remote sensing model can be applied to retrieve petroleum concentration in petroleum-contaminated water body.

Water leaving radiance (L_w) can be detected directly by visible and near infrared remote sensing sensors. R_{rs} which normalized L_w by the downwelling vector irradiance just above the sea surface, E_d (0^+), contains information about the properties of the oceanic surface layer whose thickness depends on the ocean's inherent and apparent optical properties (Stramska and Stramski, 2005; Akihiko et al, 2006). Apparently, R_{rs} not only can be used to estimate the concentrations of water constituents, but also can build links between the ocean's

inherent and apparent optical properties (Stramska et al., 2005; Akihiko et al., 2006; Huang et al., 2015;). Hence, R_{rs} is one of the primary parameters in water color remote sensing, and also is an important variable for remote sensing petroleum-pollutants.

This study concentrates on R_{rs} and relations between R_{rs} and petroleum concentration, specific absorption coefficient and specific backscattering coefficient in petroleum-contaminated water body. A survey was conducted for data collection in Dalian port, subsequently these data were preprocessed carefully for simulation tests in the study. Simulation tests were carried out by using Hydrolight, with randomly choosing of phase function, to simulate the R_{rs} spectra of pure water body and three specified petroleum-contaminated water body. Then spectral analysis and comparison methods were used here to qualitatively demonstrate their relations and to validate the feasibility of differentiating the spectra between pure water body and petroleum-contaminated water body.

2. DATA COLLECTION AND SIMULATION TEST

2.1 Data Collection

Data collection was conducted at Dalian port from August 25th to 27th, 2018. Three stations were laid out separately in this area, which was used to collect data every two meters below the sea surface from 1-meter to 15-meters in each corresponding water column and to record *in-situ* data per hour from 7:00 to 17 :00 (Figure 1). Sequentially with the calculation and interpolation of the *in-situ* data and the elimination of bad data, 15 sets of petroleum concentration, specific absorption coefficient and specific backscattering coefficient data of these stations are ready for the simulation of R_{rs} in the work.
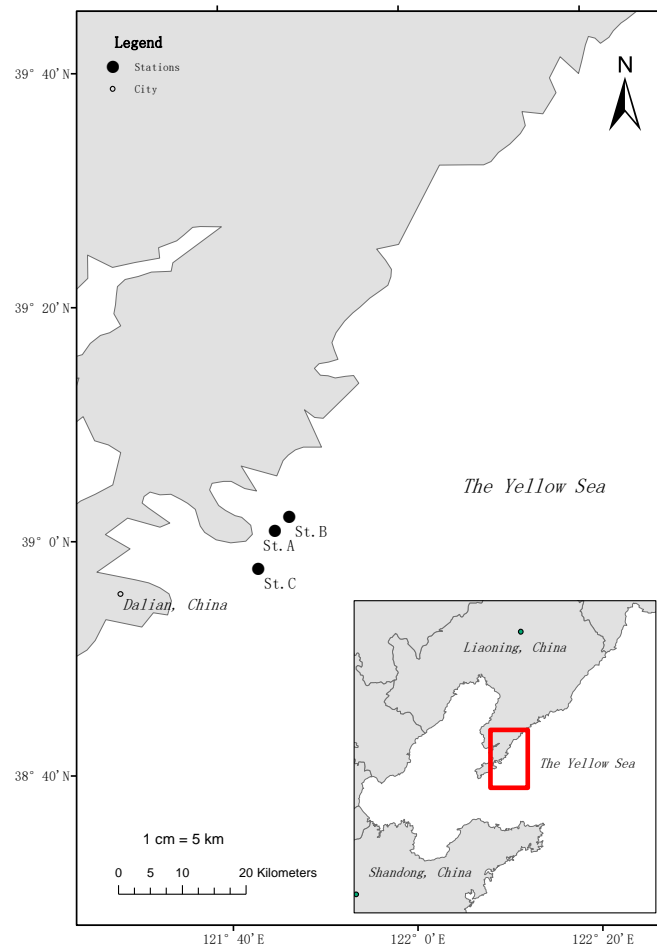

Figure 1. Locations of station for data collection in Dalian Port

2.2 Simulation Test

Randomly choose data from these 15 data sets, we design three kinds of simplified petroleum-contaminated water

2

body to simulate their R_{rs} spectra respectively by using of Hydrolight, without consideration of chlorophyll, suspended matter and colored dissolved organic matter (CDOM). For the comparability and consistency of these test results, this paper assumes that the physical environment is unchanging during the simulations. Thus, the simulations choose some default parameters, such as breezeless and cloudless daytime, standard atmosphere, marine air mass, semi-empirical sky model, infinite depth, refraction index of 1.34, zenith angle of 30°, 15m horizontal visibility, 80% humidity and 25mm precipitation. In the meantime, the simulation, who employs *avgpart* phase function of Hydrolight, also takes no account of bioluminescence and inelastic scattering in this study. For sake of convenience, the paper calls these three kinds of simulations as TEST I, TEST II and TEST III respectively in the following content.

TEST I assumed that there were 5 stations which were named as A, B, C, D and E respectively, and petroleum concentration was independent of depth, and specific absorption coefficient and specific backscattering coefficient were independent of depth and wavelength. The test fixed two parameters of petroleum concentration, specific absorption coefficient and specific backscattering coefficient as constant, and changed the remaining parameter with equal difference values in each station. It can be classified into three Modes in Test I. Such as Mode 1, Mode 2 and Mode 3. Subsequently took these data as the input of Hydrolight and randomly chose *avgpart* phase function, to simulate R_{rs} spectra and to reveal the relations between R_{rs} and petroleum concentration, specific absorption coefficient and specific backscattering coefficient. Specifically, Mode 1 set specific absorption coefficient and specific backscattering coefficient of each station as 0.0191 (m^2 mg^{-1}) and 0.1473 (m^2 mg^{-1}) respectively, and allocated petroleum concentration of each station as 5, 4, 3, 2, 1 (mg m^{-3}) separately. Mode 2 set petroleum concentration and specific backscattering coefficient of each station as 3(mg m^{-3}) and 0.1473(m^2 mg^{-1}), and allocated specific absorption coefficient as 0.0191、0.0161、0.0131、0.0101、0.0071(m^2 mg^{-1}) for each station either. Mode 3 set petroleum concentration as 3(mg m^{-3}) the same as Mode 2 and set specific absorption coefficient as 0.0191(m^2 mg^{-1}) in accordance that with Mode 1, and assigned specific backscattering coefficient of them as 0.1473、0.1173、0.0873、0.0573 and 0.0273(m^2 mg^{-1}).

TEST II also assumed that there were 5 stations which were named as A, B, C, D and E respectively as TEST I. And we also adopt the similar regime which fixed two of the three variables as constant, but chose corresponding *in-situ* data from the 15 data sets for the remaining variable. That is the remaining variable varied with depth (for petroleum concentration) or wavelength (for specific absorption coefficient and specific backscattering coefficient). TEST II also can be classified into three Modes, such as Mode 1, Mode 2 and Mode 3. Subsequently took these data as the input of Hydrolight and also chose *avgpart* phase function, to simulate R_{rs} spectra and to reveal the relations between R_{rs} and the three variables. For instance, Mode 1 set specific absorption coefficient and specific backscattering coefficient of each station as 0.0191 (m^2 mg^{-1}) and 0.1473 (m^2 mg^{-1}), and randomly chose 5 groups of petroleum concentration data from the 15 groups of *in-situ* data (Figure 2 , due to the limited space, we plotted some data in figure instead of table in the paper). Mode 2 set petroleum concentration and specific backscattering coefficient of each station as 3(mg m^{-3}) and 0.1473(m^2 mg^{-1}), and randomly chose 5 groups of specific absorption coefficient data which were shown in Figure 3 from the field dataset. Mode 3 also set petroleum concentration as 3(mg m^{-3}) and set specific absorption coefficient as 0.0191(m^2 mg^{-1}), and still randomly chose 5 groups of specific backscattering coefficient data which were shown in Figure 4 from the field dataset.
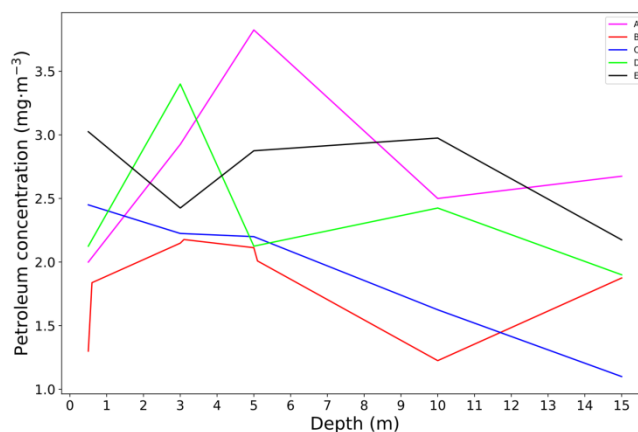

Figure 2. Petroleum concentration versus depth for Mode 1 in Test II
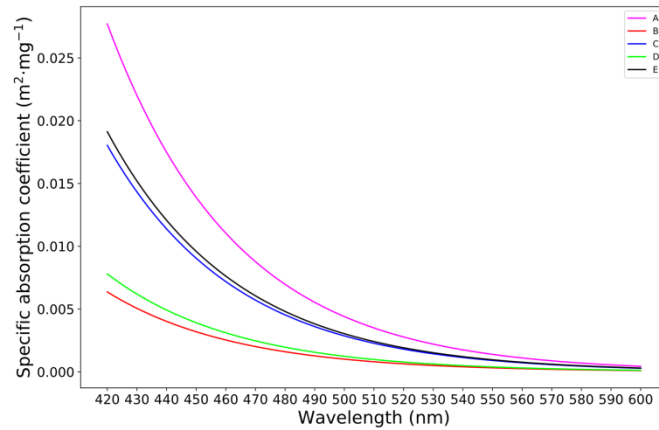
Figure 3. Specific absorption coefficient spectra for Mode 2 in Test II

Test III created 6 stations similar as TEST I, set specific absorption coefficient and specific backscattering coefficient of each station as $0.0191(m^2 \cdot mg^{-1})$ and $0.1473(m^2 \cdot mg^{-1})$ and assigned petroleum concentration of station A, B, C, D, E and F as 5, 4, 3, 2, 1, 0 (mg $\cdot m^{-3}$) respectively, in order to simulate and compare the differences of R_{rs} between petroleum-contaminated water body and pure water body. Here zero represents pure water body in station F. Petroleum concentration does not vary with depth, specific absorption coefficient and specific backscattering coefficient do not vary with wavelength either.
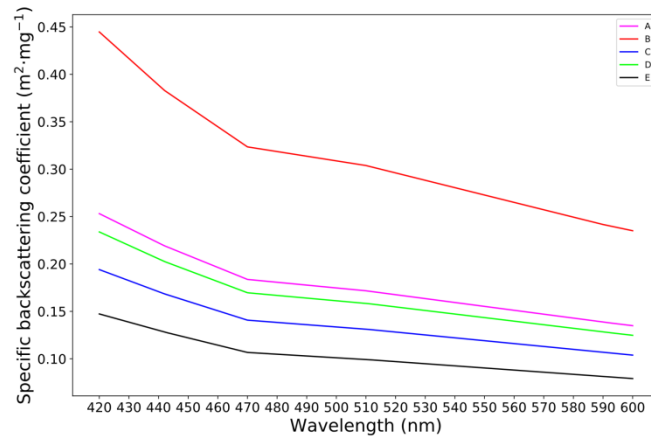

Figure 4. Specific backscattering coefficient spectra for Mode 3 in Test II

3. RESULTS AND DISCUSSION

3.1 TEST I

In TEST I, the R_{rs} spectra of Mode 1, Mode 2 and Mode 3 are shown in Figure 5, 6 and 7 respectively. Figure 5 provides insight into the relation between the R_{rs} and petroleum concentration, it shows that the R_{rs} decreases with increase of petroleum concentration in the region of 420~476nm, but increases with increase of petroleum concentration in the region of 476~600nm. In addition, R_{rs} decreases with the increase of specific absorption coefficient and increases with the increase of specific backscattering coefficient in the whole interesting spectral regions (400~600nm), as shown by the Figure 6 and Figure 7.

In a word, petroleum concentration, specific absorption coefficient and specific backscattering coefficient all can influence R_{rs} in petroleum-contaminated water body, but with different effect at different wavelength. Specifically speaking, there is negative correlation between R_{rs} and petroleum concentration between 420~476nm, and positive correlation between them from 476nm to 600nm. There is still negative correlation between R_{rs} and specific absorption coefficient and positive correlation between R_{rs} and specific backscattering coefficient in the whole spectral region.
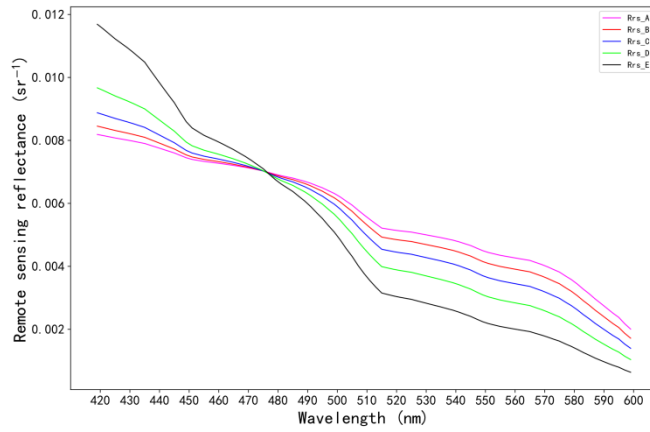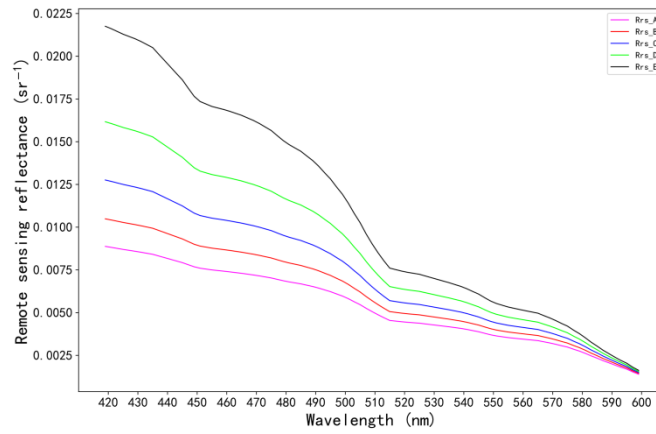
Figure 5. R_{rs} spectra of Mode 1 in Test I

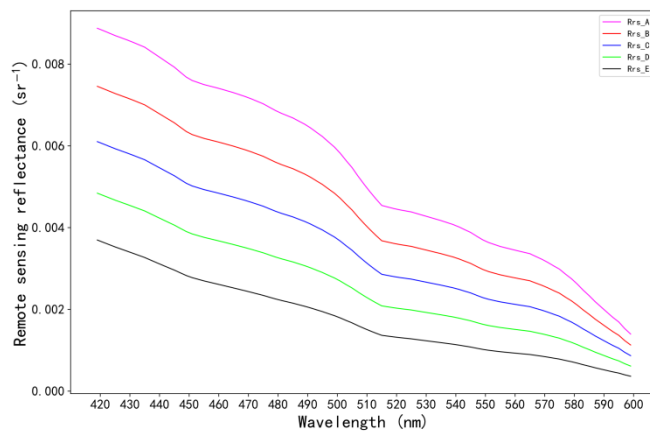Figure 6. R_{rs} spectra of Mode 2 in Test I

Figure 7. R_{rs} spectra of Mode 3 in Test I

3.2 TEST II

The R_{rs} spectra of Mode 1, Mode 2, and Mode 3 in TEST II are shown in Figure 8, Figure 9 and Figure 10.
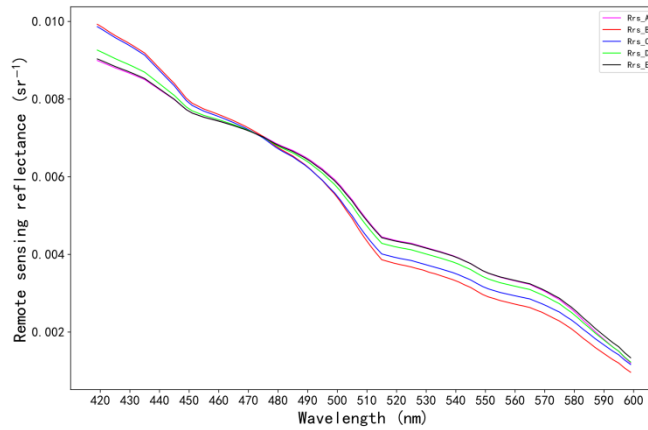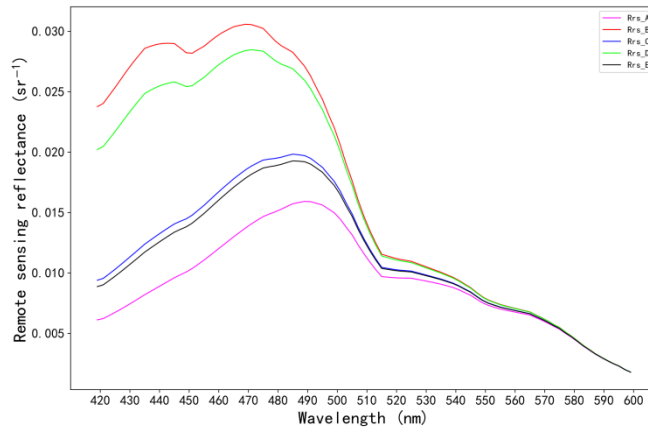
Figure 8. R_{rs} spectra of Mode 1 in Test II

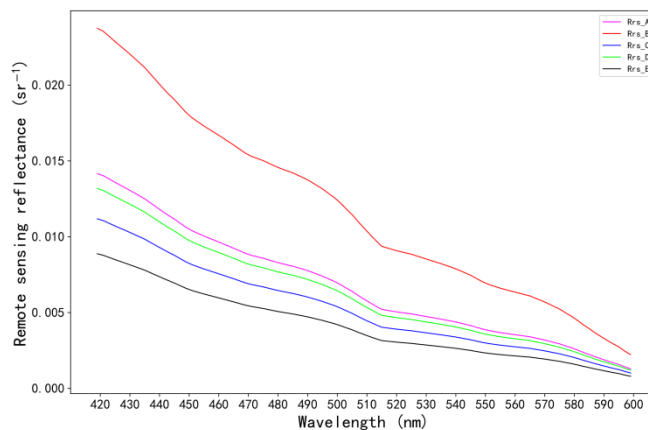Figure 9. R_{rs} spectra of Mode 2 in Test II

Figure 10. R_{rs} spectra of Mode 3 in Test II

Comparing with Figure 5, Figure 8 has similar spectra results generally. The petroleum concentration of Mode 1 in TEST II varied with depth, then the summation of petroleum concentration within corresponding water column at each station are listed in Table 1. It can be seen that Figure 8 are similar with Figure 5. Concretely speaking, R_{rs} decreases with the increase of petroleum concentration between 420~476nm and increases with the increase of petroleum concentration in the range of 476~600nm.

Table 1. Sum of petroleum concentration at each station (mg $\cdot m^{-3}$)

Station	A	B	C	D	E
Sum	418.9	252.7125	268.2125	348.2	398.725

Comparing with Figure 5, the R_{rs} spectra of station A decline quickly than those of station E when wavelength exceeds 545nm. What is more, the R_{rs} of station A are less than that of station D between 595~600nm. The difference between Figure 5 and Figure 8 indicates that there is no positive correlation between R_{rs} and petroleum concentration summation between 545nm to 600nm. Jerlov (1968), Gordon and Mccluney (1975) had verified that blue light has powerful water-penetrating capability, and the capability decreases with wavelength increasing. Besides, the capability always decreases with the concentration of particulate increasing in the water, a 'red shift' of max-penetration-band phenomenon occurs. Table 2 shows the sum of petroleum concentration of each station from sea surface to 2.5m below the sea surface. The magnitude of data in Table 2 are identical with the conclusion made by Mode 1 in Test I near 600nm. While any other sum of petroleum concentration has no positive correlation with R_{rs} at 600nm. So only petroleum-pollutants who distributed less than 2.5m depth could have obvious influence on R_{rs} at 600nm. On the other hand, those petroleum-pollutants who distributed more than 2.5m could make little contribution to R_{rs} at 600nm due to the penetrating ability of light or the absorption of petroleum particles.

Table 2. The sum of petroleum concentration from sea surface to
depth of 2.5m below the sea surface (mg $\cdot m^{-3}$)

Station	A	B	C	D	E
Sum	49.77	40.5195	49.56	55.335	58.485

Figure 9 shows that the R_{rs} decreases with the increasing of specific absorption coefficient in the whole spectral region, the same as Figure 6 shows. We encoded a ranking program with Python to order the magnitude of specific absorption coefficient for each station of Mode 2 in TEST II in each wavelength. The ranking results in each wavelength all have same order, and are listed in Table 3. However, Figure 9 has a single hump between 420nm to 515nm, Figure 6 has not. The difference between them indicates that the specific absorption coefficient can influence R_{rs} more significant than petroleum concentration and specific backscattering coefficient.

Table 3. Ranking order of specific absorption coefficient (A > E > C > D > B)

Station	A	B	C	D	E
Order	4	0	2	1	3

Figure 10 shows the same results as Figure 7, that is R_{rs} increases with the increase of specific backscattering coefficient between 420nm to 600nm. We also did a ranking work for the magnitude of specific backscattering coefficient of each station for Mode 3 in TEST II in every wavelength and the ranking results in each wavelength are same either. The results are listed in Table 4.

Table 4. Ranking order of specific backscattering coefficient (B > A > D > C > E)

Station	A	B	C	D	E
Order	3	4	1	2	0

TEST II made further efforts to prove that the conclusions of TEST I are correct, and it also pointed out that only petroleum particles distributed in the water surface (about less than 2.5m depth) could influence the R_{rs} near 600nm, due to the penetrating ability of light decreases with wavelength increasing, while those petroleum particles distributed deeper than 2.5m would have little influence on R_{rs} at 600nm. Furthermore, TEST II still indicated that specific absorption coefficient is more important than petroleum concentration and specific backscattering coefficient for R_{rs}.

3.3 TEST III

The R_{rs} spectra of TEST III are shown in Figure 11, and it shows that the difference of R_{rs} between pure water body and petroleum-contaminated water body are obvious, especially at blue band. Similarly, green band also can be used for the differentiating of pure water body and petroleum-contaminated water body.
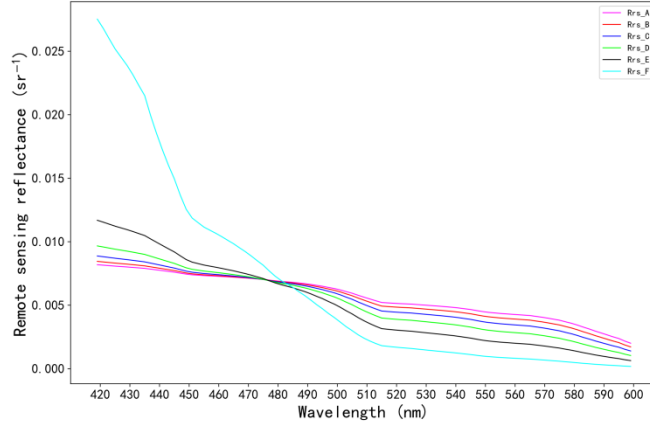
Figure 11. R_{rs} spectra in Test III

Moreover, normalized R_{rs} could be used for the differentiating of pure water body and petroleum-contaminated water body effectively for *in-situ* data and remote sensing data (Huang et al., 2016). Normalized R_{rs} is defined in Equation (1).

$$R'_{rs} = \frac{R_{rs,i}}{\Sigma_{i=1}^{n} R_{rs,i}} \tag{1}$$

Where R'_{rs} is the normalized R_{rs}, $R_{rs,i}$ is the R_{rs} at i^{th} band (Huang et al., 2016). The paper plotted normalized R_{rs} spectra of pure water body and petroleum-contaminated water body as well (Figure 12). Apparently the normalized R_{rs} of pure water body and petroleum-contaminated water body can be distinguished more easily than R_{rs} of them. Figure 12 also shows that 'blue shift' of pure water body occurs. This 'blue shift' of pure water body on normalized R_{rs} spectra lead us to re-find the 'red shift' of pure water body in Figure 11.
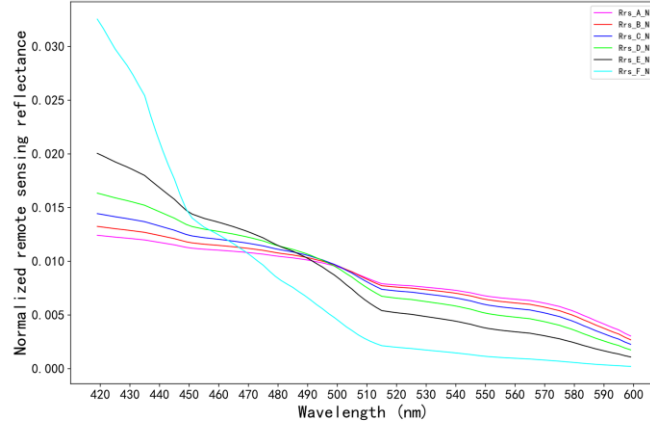

Figure 12. Normalized R_{rs} spectra in Test III

In this paper the simulation of each TEST considered that the physical environment was unchanging, so the downwelling irradiance just above the sea surface ($E_d(0_+)$) was unchanging either. So, Equation (2) indicates that only water-leaving radiance (L_w) can influence the R_{rs}.

$$R_{rs} = \frac{L_w}{E_d(0_+)} \tag{2}$$

The L_w spectra in TEST III are shown in Figure 13. The spectra of Figure 13 have the similar shape as those of Figure 11, L_w in Figure 13 and R_{rs} in Figure 11 both has same correlation with petroleum concentration. Thus, the 'red shift' in Figure 11 must be caused by that in Figure 13. In addition, Figure 13 shows that L_w of petroleum-contaminated water body are not dependent on petroleum concentration at 476nm, and L_w of pure water body are slightly higher than that of petroleum-contaminated water body. For this reason, the difference of L_w

between pure water body and petroleum-contaminated water body at 476nm induces the 'blue shift' of normalized R_{rs} of pure water body in Figure 12, it also makes the difference of normalized R_{rs} between pure water body and petroleum-contaminated water body more clearly at green band.
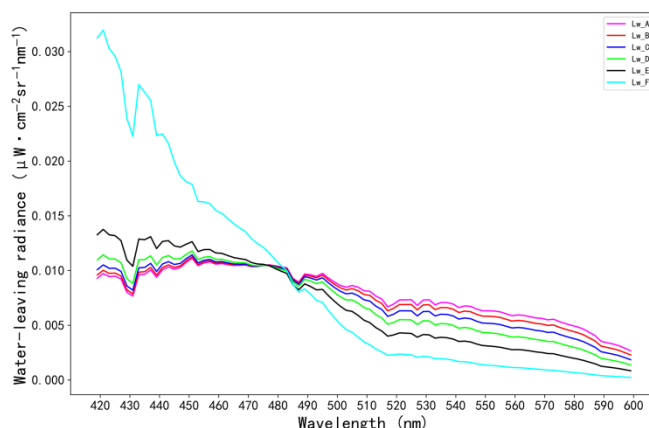

Figure 13. L_w spectra in Test III

4. CONCLUSIONS

In this study, we designed three kinds of simulation to build links between R_{rs} and petroleum concentration, specific absorption coefficient and specific backscattering coefficient. TEST I and TEST II together reveal that petroleum concentration, specific absorption coefficient and specific backscattering coefficient could influence R_{rs} in petroleum-contaminated water body, but in different way. Such as R_{rs} decreases with petroleum concentration increasing between 420nm to 476nm and increases with its concentration increasing in the spectral region of 476~600nm. And there is still negative correlation between R_{rs} and specific absorption coefficient and positive correlation between R_{rs} and specific backscattering coefficient in the whole spectral region (420~600nm).

Moreover, TEST II makes further efforts to demonstrate that specific absorption coefficient is more important than petroleum concentration and specific backscattering coefficient, especially at blue band, for the reason that the slightly change of specific absorption coefficient can bring about changes for the shape of R_{rs} spectra. It also reveals that the green and yellow band of light has weak ability to penetrate water between 545nm to 600nm. Especially nearby 600nm, only petroleum particles distributed in the sea surface water column could influence R_{rs} in petroleum-contaminated water body, while the petroleum particles distributed in the deeper water column could influence R_{rs} as well at blue band.

At last, TEST III validated that R_{rs} of pure water body and petroleum-contaminated water body could be differentiated at blue and green band. In addition, normalized R_{rs} could distinguish them more efficiently than R_{rs}, especially at green band. The normalized R_{rs} spectra still shows a particular 'blue shift' phenomenon, and it also helped us re-find a slightly 'red-shift' of pure water body occurred in R_{rs} spectra. Finally, a conclusion that the 'blue-shift' phenomenon and the better differentiating ability of normalized R_{rs} are both caused by the 'red shift' of pure water body in L_w spectra.

REFERENCS

Akihiko, T., Hiroaki, S. and Joji, I., 2006. Alternative measuring method for water-leaving radiance using a radiance sensor with a domed cover. Optics Express, 14(8): pp. 3099-3105.
Gordon, H., Mccluney, W., 1975. Estimation of The Depth of Sunlight penetration in The Sea for Remote Sensing. Applied Optics, 14(2). pp. 413-416.

Huang, M.F., Li, X.X., Bai, Z.A., Qin, F.Y., Hou, R.B. and Wang, L., 2009. Water spectral absorption features of petroleum pollution in middle infrared bands. Arid Land Geography, 32 (1), pp. 139-144.

Huang, M.F., Song, Q.J. and Jian, W.J., 2012. The retrieval model for petroleum concentration in waters using remote sensing data. Acta Oceanologica Sinica, 34 (5), pp. 74-80.

Huang, M.F., Song, Q.J. and Chen, L.B., 2015. Research on an Inverse Model of Petroleum Content in Water Bodies Based on the Normalized Remote sensing Reflectance. Journal of Ocean Technology, 34 (1), pp. 1-9.

Huang, M.F., Song, Q.J., Xing, X.F. and Liu, Y., 2016. Remote Sensing Detection Mechanism and Information Extraction Method of Water Petroleum Pollution. Science Press, Beijing. pp.1-5.

Jerlov, N.G., 1968. Optical Oceanography. Elsevier, Amsterdam, pp. 167-168.

Król, T., Stelmaszewski, A. and Freda, W., 2006. Variability in the optical properties of a crude oil - seawater emulsion. Oceanologia, 48 (S), pp. 203-211.

Novo et al., 1991. Results of a Laboratory Experiment Relating Spectral Reflectance to Total Suspended Solids. Remote Sens. Environ., 36, pp. 67-72.

Stramska, M. and Stramski, D., 2005. Effects of a nonuniform vertical profile of chlorophyll concentration on remote-sensing reflectance of the ocean. Applied Optics., 44(9), pp. 1735-1747.

Tan, Q.L. and Shao, Y., 2000. Application of Remote Sensing Technology to Environmental Pollution Monitoring. Remote Sensing Technology and Application, 15 (4), pp. 246-251.

Wozniak, S.B. and Stramski, D., 2004. Modeling the optical properties of mineral particles suspended in seawater and their influence on ocean reflectance and chlorophyll estimation from remote sensing algorithms. Applied Optics, 43 (17), pp. 3489-3503.